Experimental Studies of Deeply Virtual Compton Scattering at JLab

F.-X. Girod

JLab Hall-B

HUGS 2012

Experimental studies at 6 GeV

Pioneering observations

First DVCS BSA and TSA observations

$A_{LU} \propto F_1\mathcal{H} + \xi G_M\tilde{\mathcal{H}} - \frac{t}{4M^2}F_2\mathcal{E}$

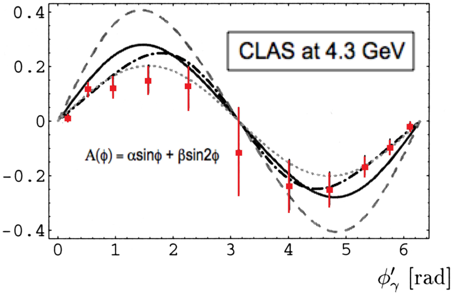

$Q^2 = 1.3$ GeV^2, $x_B = 0.2$, $-t = 0.2$ GeV^2

$$\begin{aligned} A(\phi) &= \alpha \sin\phi + \beta\cos(2\phi) \\ \alpha &= 0.202 \pm 0.028^{stat} \pm 0.013^{syst} \\ \beta &= -0.024 \pm 0.021^{stat} \pm 0.009^{syst} \end{aligned}$$

S. Stepanyan *at al.*, PRL **87** (2001) 182002

250+ citations

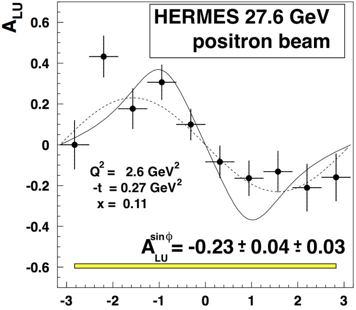

$A_{UL} \propto F_1\tilde{\mathcal{H}} + \xi G_M\left(\mathcal{H} + \frac{\xi}{1+\xi}\mathcal{E}\right) - \cdots$

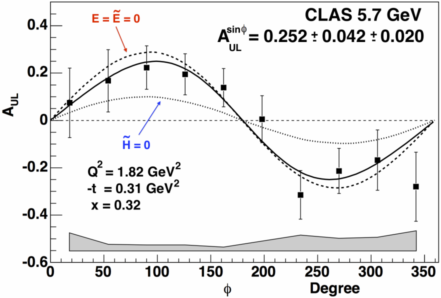

Pioneering observations
First DVCS BSA observations

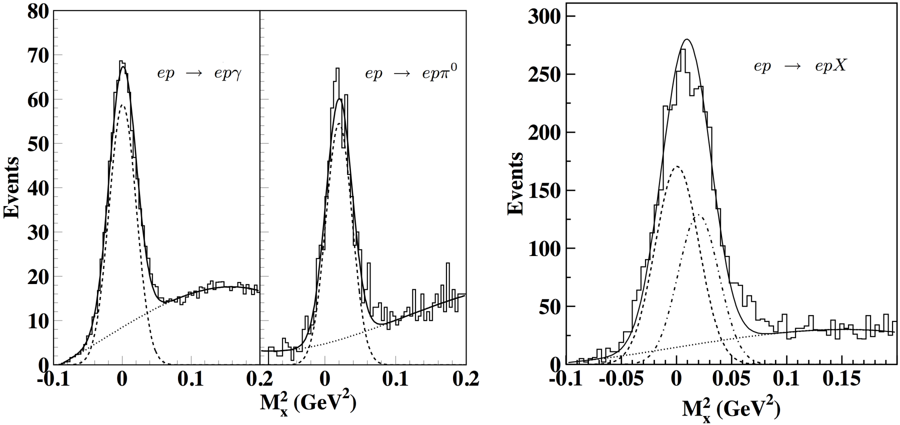

Pioneering observations

First DVCS TSA observations

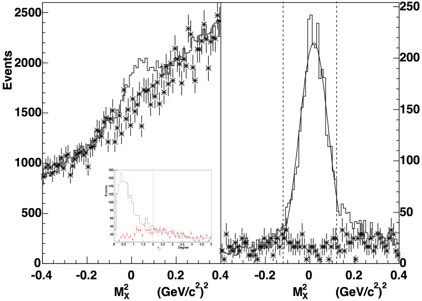

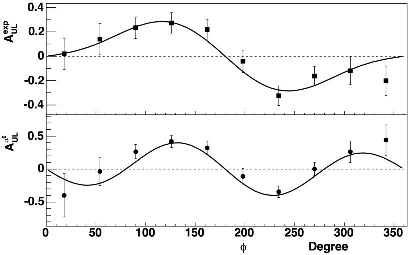

Scaling tests of $\Delta\sigma_{\text{DVCS}}$ E00-110

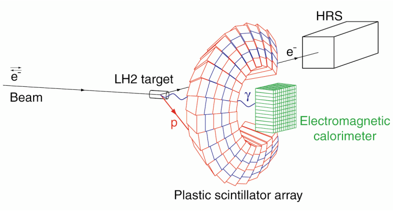

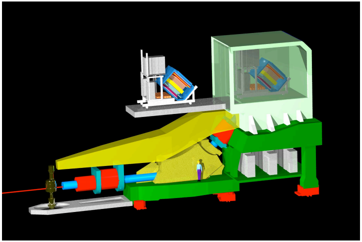

100-channel scintillator array

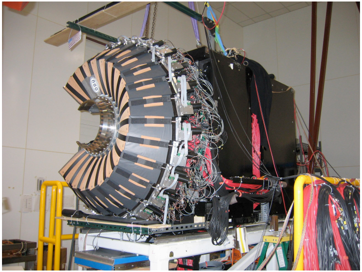

132-block PbF_2 electromagnetic calorimeter

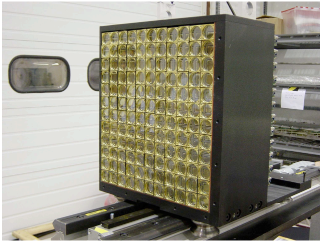

Scaling tests of $\Delta\sigma_{\mathrm{DVCS}}$ E00-110

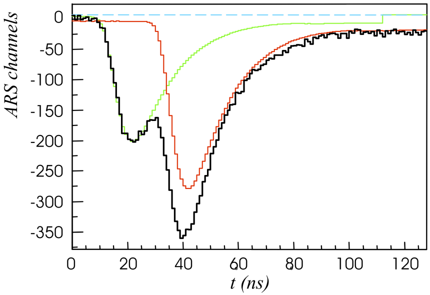

Analog Ring Sampler
Quasi-continuous scan of amplitude
128 samples 1 GHz
Included in trigger LOT
Separated pile-up

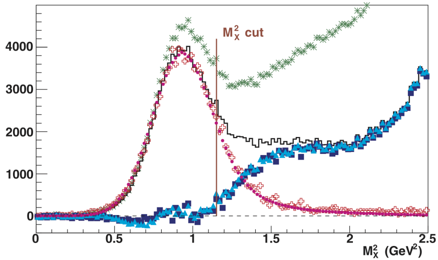

Missing-mass very clean
Inelastic background under control

Scaling tests of $\Delta\sigma_{\mathrm{DVCS}}$ E00-110

$$F_1\mathcal{H} + \xi G_M\tilde{\mathcal{H}} - F_2\frac{t}{4M^2}\mathcal{E} + \cdots$$

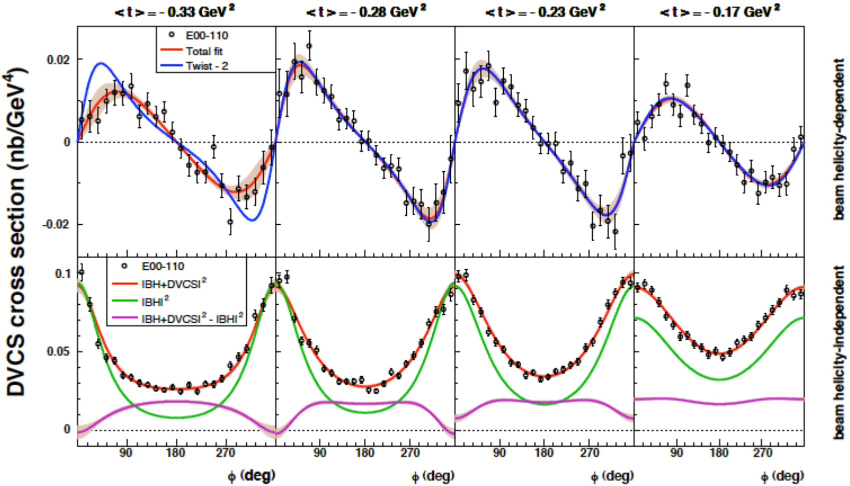

Separation of $\mathcal{I}$ and DVCS^2 E00-110/E07-007

$$F_1 \mathcal{H} + \xi G_M \tilde{\mathcal{H}} - F_2 \frac{t}{4M^2} \mathcal{E} + \cdots$$

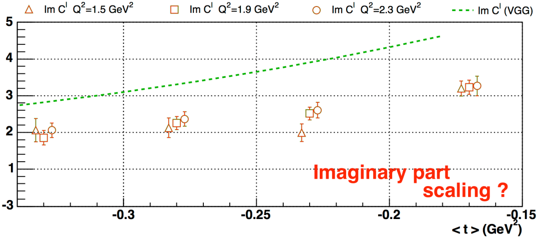

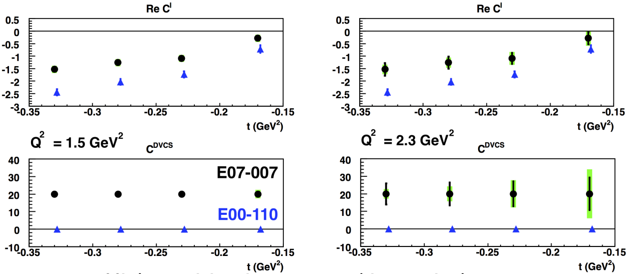

High precision in a narrow kinematical range

Preliminary analysis demonstrates that the experiment was running well:

- 2-γ invariant mass reproduces the π^0
- ep $\rightarrow e\gamma x$ has the desired peak at the nucleon mass, and
- the ep $\rightarrow$ ep elastic calibration reproduces the expected energy resolution

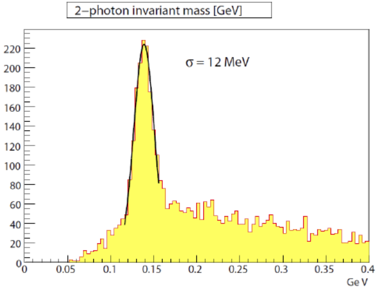

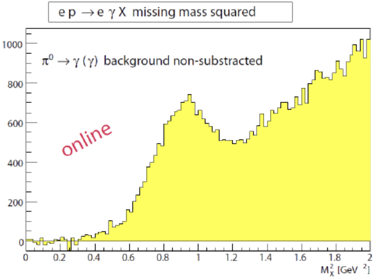

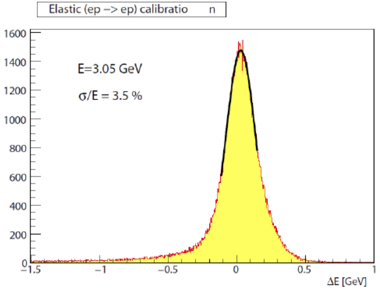

Neutron DVCS E03-106

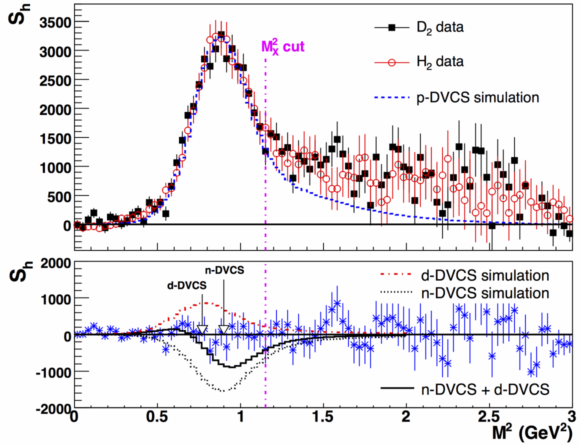

Separation of H and D helicity signals
Proton data smeared Fermi motion
Spectrum after subtraction fitted with simulation

M. Mazouz *et al.*, PRL **99** (2007) 242501

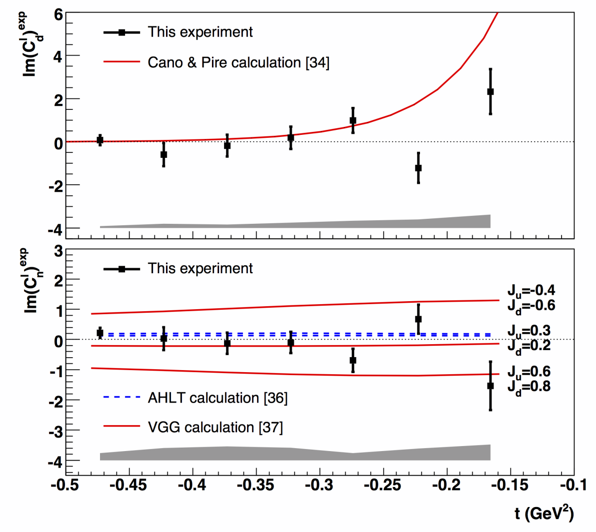

t-dependence
sinϕ moment
coherent (top)
incoherent (bottom)

M. Mazouz *et al.*, PRL **99** (2007) 242501

Neutron DVCS E03-106

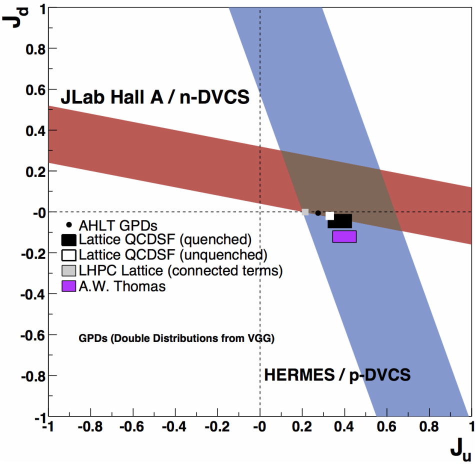

Model dependent extraction

M. Mazouz *et al.*, PRL **99** (2007) 242501

lattice: QCDSF

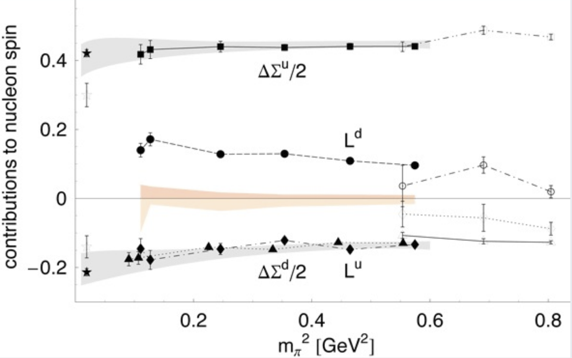

- no disconnected quark loops
- chiral extrapolation

$$J^q = \frac{1}{2}\int dx\, x\,[H(x,0,0) + E(x,0,0)] \qquad L^q = J^q - \frac{1}{2}\Delta\Sigma^q$$

CLAS in Hall-B

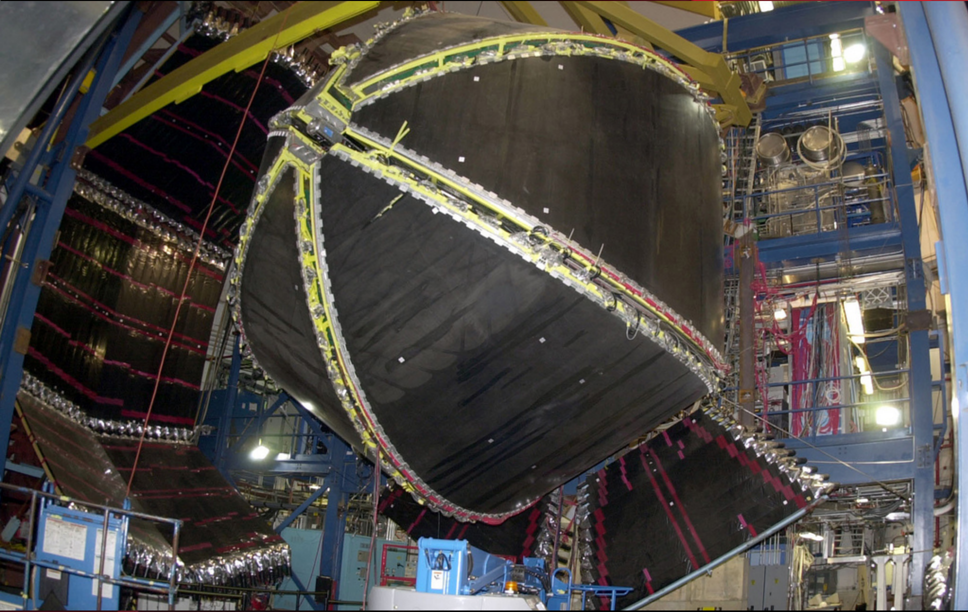

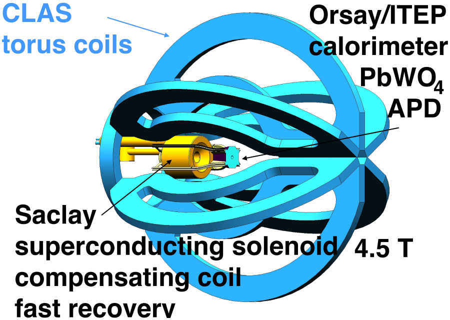

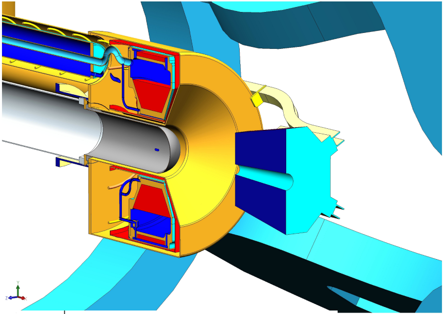

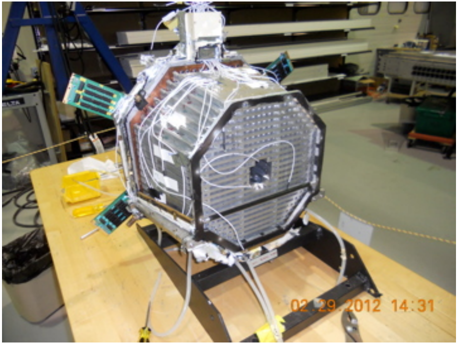

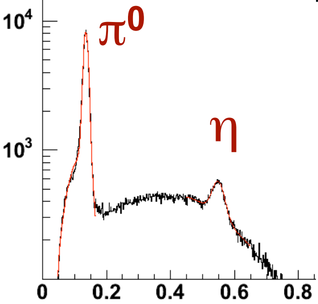

$$M_{\gamma\gamma} = \sqrt{2E_{\gamma_1}E_{\gamma_2}\left(1-\cos\theta_{\gamma\gamma}\right)}$$

Solenoid and Inner Calorimeter

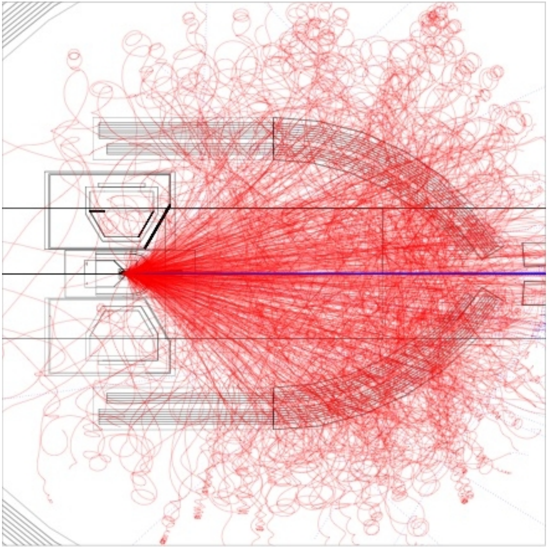

Solenoid and Inner Calorimeter

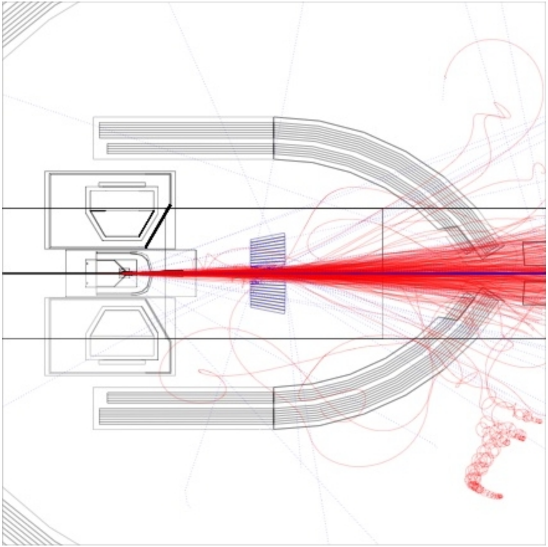

Flavor of analysis

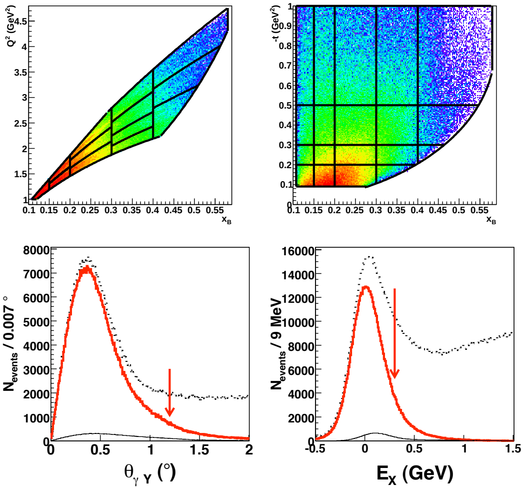

- kinematical coverage
- exclusivity cuts
- π^0 subtraction

CLAS proton Beam Spin Asymmetry E01-113

$$F_1\mathcal{H} + \xi G_M\tilde{\mathcal{H}} - \frac{t}{4M^2}F_2\mathcal{E}$$

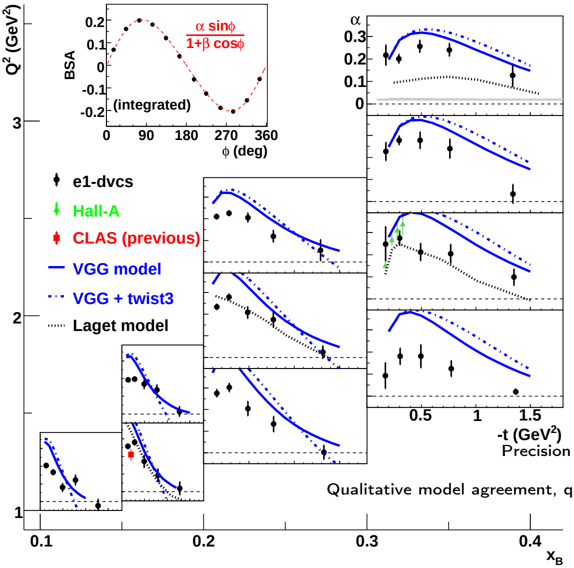

Precision in a large phase-space (x_B, Q^2, t)

Qualitative model agreement, quantitative constraints on parameters

F.-X. G. *et al.*, PRL **100** (2008) 162002

CLAS proton cross-section

E01-113

$$F_1\mathcal{H} + \xi G_M\tilde{\mathcal{H}} - \frac{t}{4M^2}F_2\mathcal{E}$$

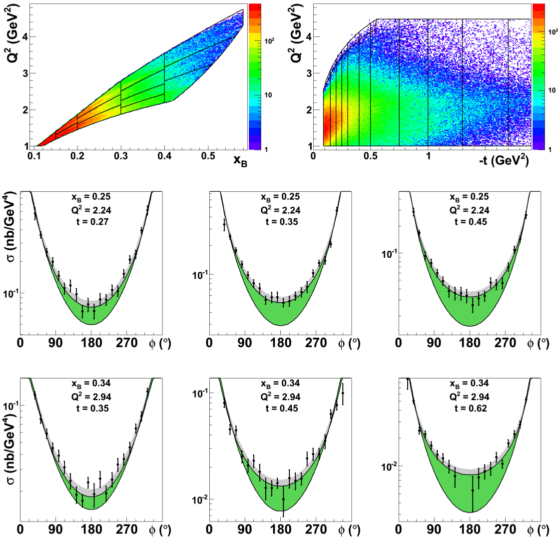

More than 3k bins

Dispersion relation :

$$\mathcal{R}e\ \mathcal{H} = \left[\int \mathcal{I}m\ \mathcal{H}\right] + \mathcal{D}$$

green band shows difference with BH

$\rightarrow$ sensitivity to d_1

DVCS cross-section analysis

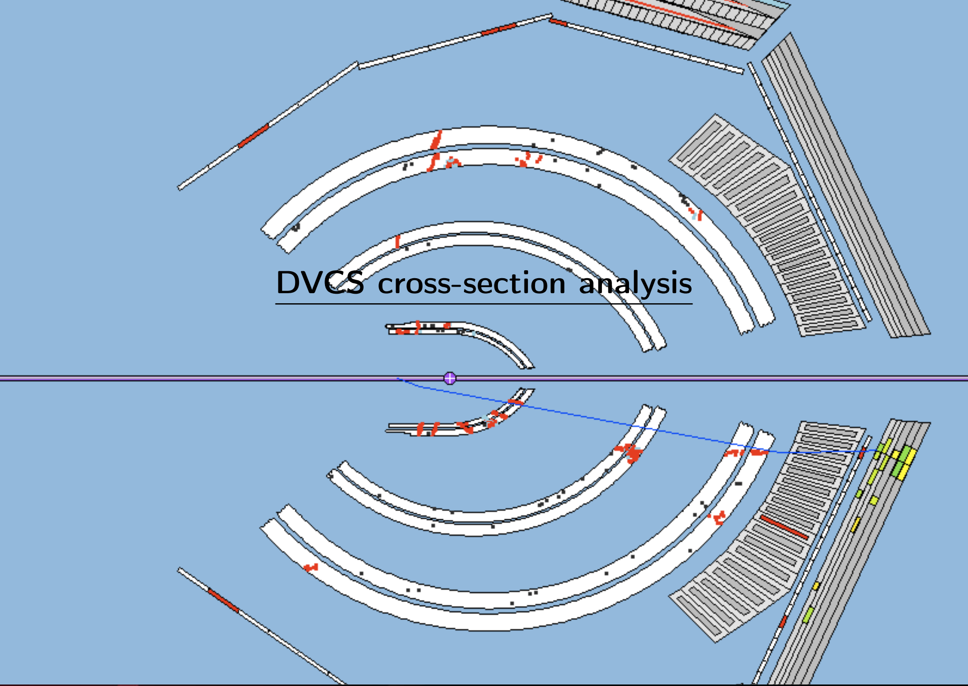

Random background and efficiencies

Illustration of lost electron track :

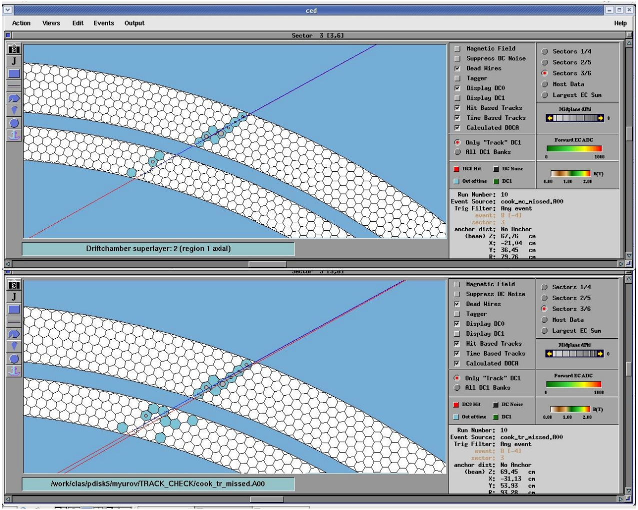

Random background and efficiencies

Quantitative conclusions :

Merging the background from data with simulation results in $\approx 30\%$

(1)	Not reconstructed	1.8%
(2)	stat[0]>0 cut	74.5%
(3)	ecsfr cut	0.9%
(4)	nphe>25 cut	4.7%
(5)	ficudial cut	0.9%
(6)	stat>0 (others)	14.4%
(7)	charge>0	1.8%
(8)	id==2212 cut	0.9%

Electron recovery procedure
Search for matching TB track with CC hit
Data : 9.4%
MC : 10.8%
remarquable test of consistency
Trigger recovery procedure
$\approx 5\%$

Final background correction $\approx 15\%$

Radiative corrections
Diagrammatics

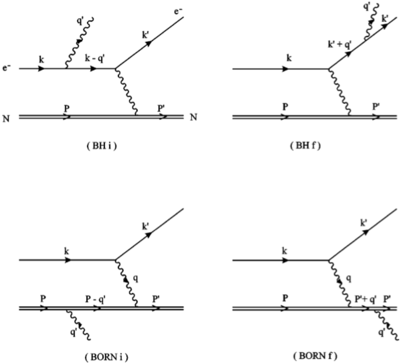

Radiative corrections

Summary : who ordered them ?

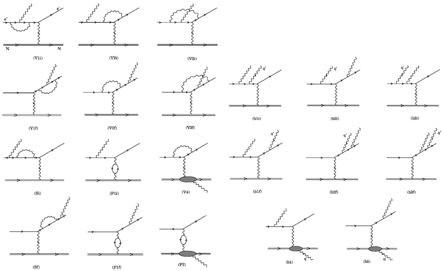

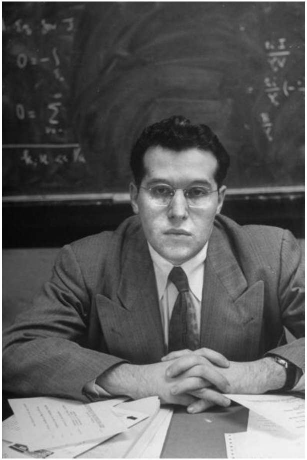

M. Vanderhaeghen *et al.*, Phys. Rev **C62** (200) 025510

First order radiative corrections

Another convenient factorization theorem

$$
\begin{aligned}
\left.\frac{\mathrm{d}\sigma}{\mathrm{d}\Omega}\right|_{\mathrm{exp}} &= \left.\frac{\mathrm{d}\sigma}{\mathrm{d}\Omega}\right|_{\mathrm{Virtual}\ \gamma} + \left.\frac{\mathrm{d}\sigma}{\mathrm{d}\Omega}\right|_{\mathrm{Real}\ \gamma} \\
&= \left.\frac{\mathrm{d}\sigma}{\mathrm{d}\Omega}\right|_{\mathrm{Born}} \left[1 + \delta_{\mathrm{Vertex}} + \delta_{\mathrm{Vacuum}} + \delta_{\mathrm{Real}}(\Delta E)\right]
\end{aligned}
$$

First order radiative corrections

Expressions for the virtual and real corrections

$$\delta_{\text{Vacuum}} = \frac{2\alpha}{3\pi}\left[\ln\left(\frac{Q^2}{m_e^2}\right) - \frac{5}{3}\right] + \infty$$

$$\delta_{\text{Vertex}} = \frac{\alpha}{\pi}\left[\frac{3}{2}\ln\left(\frac{Q^2}{m_e^2}\right) - 2 - \frac{1}{2}\ln^2\left(\frac{Q^2}{m_e^2}\right) + \frac{\pi^2}{6}\right] + \infty$$

$$\delta_{\text{Real}}(\Delta E) = \frac{\alpha}{\pi}\left\{2\ln\left(\frac{\Delta E}{\sqrt{EE'}}\right)\left[\ln\left(\frac{Q^2}{m_e^2}\right) - 1\right] - \frac{1}{2}\ln^2\frac{E}{E'} + \frac{1}{2}\ln^2\left(\frac{Q^2}{m_e^2}\right) - \frac{\pi^2}{3} + \text{Sp}\left(\cos^2\frac{\theta_e}{2}\right)\right\} + \infty$$

$\delta_{\text{Vertex}} + \delta_{\text{Vacuum}} + \delta_{\text{Real}}(\Delta E)$ finite

All order resummation

Bloch & Nordsieck's magic

$$\left.\frac{d\sigma}{d\Omega}\right|_{exp} = \left.\frac{d\sigma}{d\Omega}\right|_{Born} \frac{e^{\delta_{Vertex}+\delta^0_{Real}}}{(1-\delta_{Vacuum}/2)^2}\left(\frac{\Delta E}{\sqrt{EE'}}\right)^{\delta_S}$$

$$\delta_S = \frac{2\alpha}{\pi}\left[\ln\left(\frac{Q^2}{m_e^2}\right)-1\right]$$

δ_S defining the radiative lineshape (soft-photon approximation) (soft-photon approximation) is integrated through fast-MC, in order to properly convolute with the 5-fold acceptance.

N.B.: This already is only justified in the peaking approximation

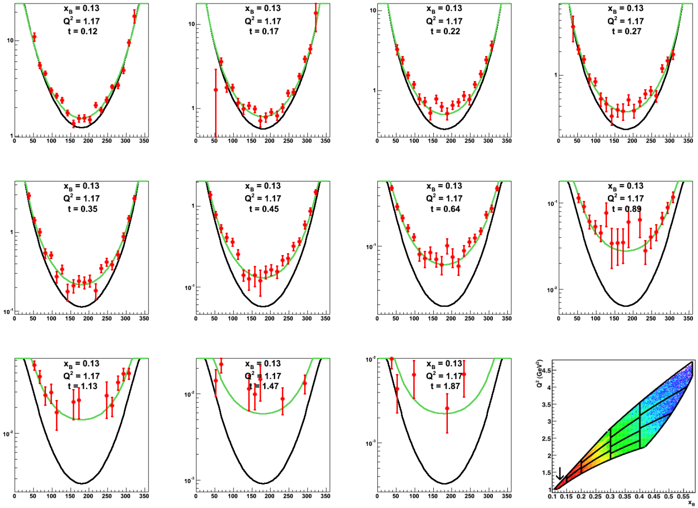

x_B = 0.13
Q^2 = 1.17
t = 0.12
x_B = 0.13
Q^2 = 1.17
t = 0.17
x_B = 0.13
Q^2 = 1.17
t = 0.22
x_B = 0.13
Q^2 = 1.17
t = 0.27
x_B = 0.13
Q^2 = 1.17
t = 0.35
x_B = 0.13
Q^2 = 1.17
t = 0.45
x_B = 0.13
Q^2 = 1.17
t = 0.64
x_B = 0.13
Q^2 = 1.17
t = 0.89
x_B = 0.13
Q^2 = 1.17
t = 1.13
x_B = 0.13
Q^2 = 1.17
t = 1.47
x_B = 0.13
Q^2 = 1.17
t = 1.87
Q^2 (GeV^2)
x_B

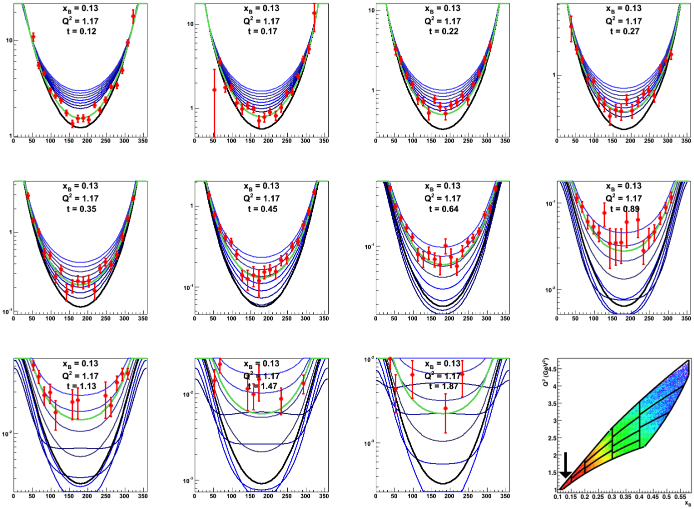

x_B = 0.13
Q^2 = 1.17
t = 0.12
x_B = 0.13
Q^2 = 1.17
t = 0.17
x_B = 0.13
Q^2 = 1.17
t = 0.22
x_B = 0.13
Q^2 = 1.17
t = 0.27
x_B = 0.13
Q^2 = 1.17
t = 0.35
x_B = 0.13
Q^2 = 1.17
t = 0.45
x_B = 0.13
Q^2 = 1.17
t = 0.64
x_B = 0.13
Q^2 = 1.17
t = 0.89
x_B = 0.13
Q^2 = 1.17
t = 1.13
x_B = 0.13
Q^2 = 1.17
t = 1.47
x_B = 0.13
Q^2 = 1.17
t = 1.87
Q^2 (GeV^2)
x_B

NMR Measurement

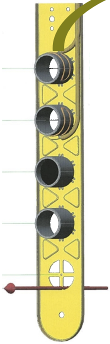

- ➢ $^{14}NH_3$ target material
- ➢ Cooled to ~ 1 Kelvin using evaporative cooling on LHe
- ➢ Surrounded by a 5 Tesla superconducting magnet
- ➢ Continuously polarized using Dynamic Nuclear Polarization (DNP)
- ➢ Polarization during the experiment was monitored by Nuclear Magnetic Resonance (NMR) measurement →

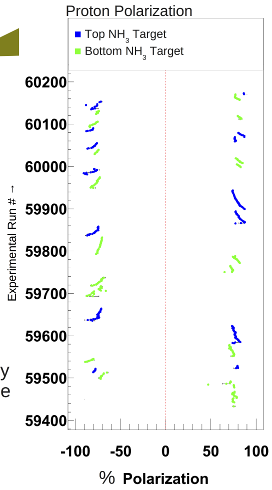

- ➢ The target insert (shown above left) held 4 targets for use in the eg1-dvcs experiment: 2 polarized NH_3 targets, 1 carbon target, and 1 empty target cup.

- ➢ Average achieved proton longitudinal polarization ~ 85%.

CLAS proton Target Spin Asymmetry E05-114

Ten fold improvement in statistics

$$F_1 \tilde{\mathcal{H}} + \xi G_M \left(\mathcal{H} + \frac{\xi}{1+\xi} \mathcal{E} \right)$$

$A_{UL} \propto F_1 \, \mathcal{I}m \, \tilde{\mathcal{H}}$ $\qquad$ $A_{LL} \propto F_1 \, \mathcal{R}e \, \tilde{\mathcal{H}}$

Pioneering observations

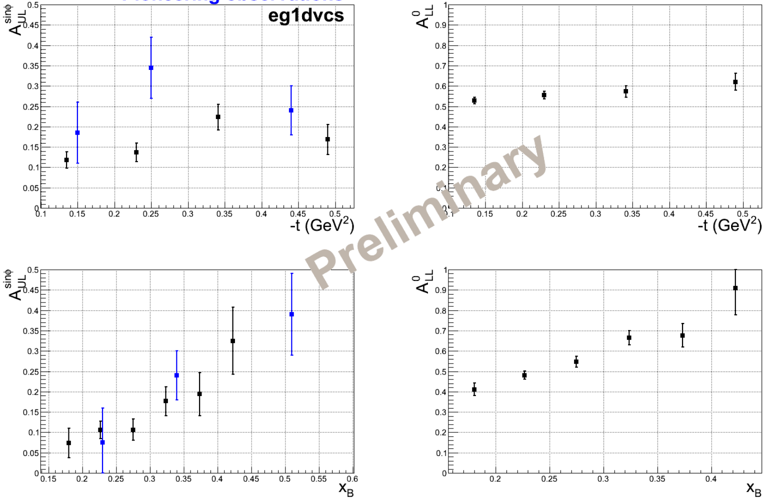

DD+D MMS model

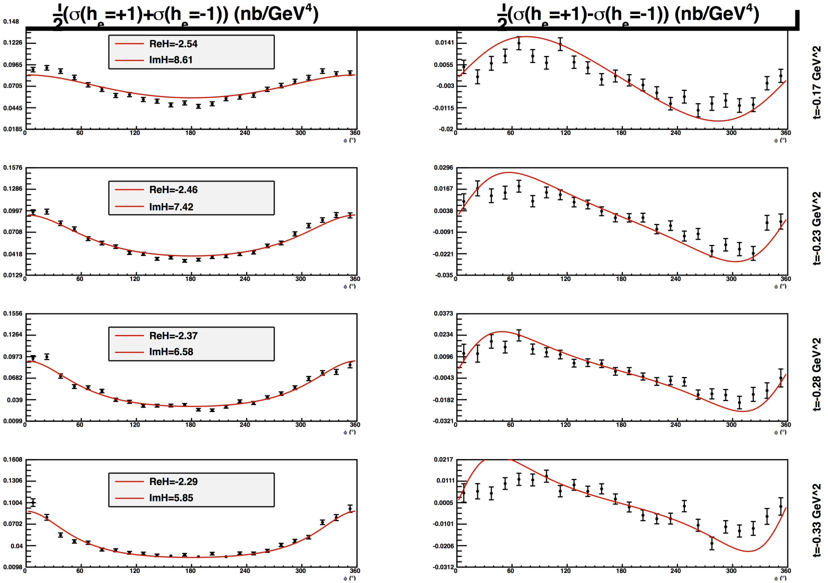

Extraction results

KMa/b : Kumerički and Müller, Nucl. Phys. B841 (2010)
Guidal : Phys.Lett. B689 (2010) 156
Phys.Lett. B693 (2010) 17
Moutarde : Phys. Rev. D79, 094021 (2009)

Local fits of DVCS :
fits of Re and Im parts of Compton Form Factors

Global fits of DVCS :
fits to parametrized GPD models

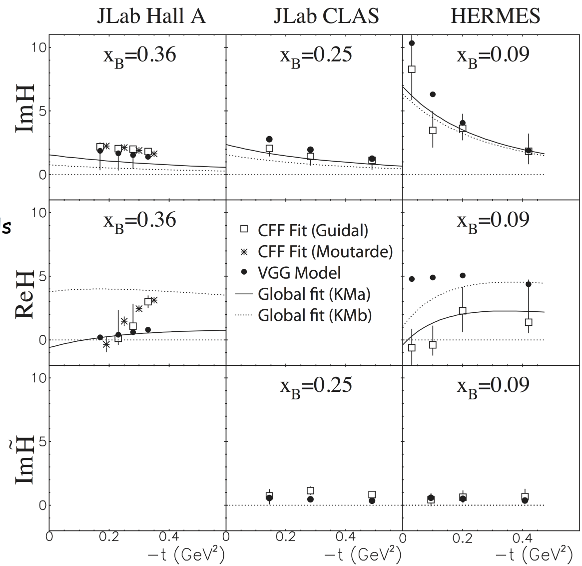

Findings :
Slope of ImH ↗ when x_B ↘

Accurate cross section data drive global fits to use more than just GPD H

Im$\tilde{H}$ seems to have weak t and x_B dependence

Model independent extraction

Using only A_{LU} and A_{UL}

Extraction with :

- Preliminary results from eg1dvcs A_{UL}
- Polarized cross-section from e1dvcs $\Delta\sigma$

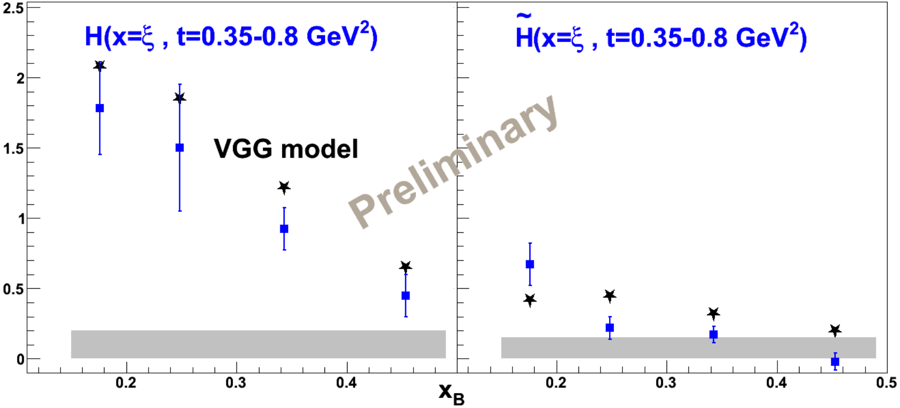

GPD dependencies versus x_B mirror their respective ordinary PDFs

$\tilde{H}$ and $H \leftrightarrow \Delta q(x)$ and $q(x)$

Drop of $\Delta q(x)$ at low x_B will be seen at 12 GeV

6 GeV era : lessons learned

- The feasibility of high luminosity exclusive measurements in complementary high precision (Hall-A) and large acceptance (CLAS) spectrometers has been demonstrated.
- The first dedicated generation of experiments suggests precocious scaling in Deeply Virtual Compton Scattering
- The experimental results have triggered theoretical developments for the consistent description of higher twist corrections
- Several approaches investigate Generalized Parton Distribution extraction methods from data
- Unified descriptions with Semi-Inclusive DIS in terms of Wigner distributions have recently been implemented into concrete predictions